RAPID COMMUNICATIONS

PHYSICAL REVIEW C

NUCLEAR PHYSICS

THIRD SERIES, VOLUME 52, NUMBER 3 SEPTEMBER 1995

RAPID COMMUNICATIONS

The Rapid Communications section is intended for the accelerated publication of important new results. Manuscripts submitted to this section are given priority in handling in the editorial office and in production. A Rapid Communication in **Physical Review C** *may be no longer than five printed pages and must be accompanied by an abstract. Page proofs are sent to authors.*

The $^{12}C(\gamma,K^+)$ reaction in the threshold region

H. Yamazaki,[1] K. Maeda,[2] S. Asano,[3,*] T. Emura,[4] S. Endo,[3,†] S. Ito,[1] H. Itoh,[1] O. Konno,[1] K. Maruyama,[5] K. Niwa,[4] A. Sakaguchi,[3] T. Suda,[2] Y. Sumi,[3] M. Takeya,[1,‡] T. Terasawa,[1] and H. Yamashita[4]

[1]*Laboratory of Nuclear Science, Tohoku University, Sendai 982, Japan*

[2]*Department of Physics, Tohoku University, Sendai 980-77, Japan*

[3]*Department of Physics, Hiroshima University, Higashi-Hiroshima 724, Japan*

[4]*Department of Applied Physics, Tokyo University of Agriculture and Technology, Koganei, Tokyo 184, Japan*

[5]*Institute for Nuclear Study, University of Tokyo, Tanashi, Tokyo 188, Japan*

(Received 26 September 1994)

The first measurement of $^{12}C(\gamma,K^+)$ has been performed in a photon energy range of $0.8 \leq E_\gamma \leq 1.1$ GeV. The differential cross sections are compared with a calculation which assumes a quasifree Λ-producing $^{12}C(\gamma,K^+)$ process. The deviation of experimental values from the calculation is explained in terms of bound Λ residual states. The differential cross section ratio of $^{12}C(\gamma,K^+)$ to $p(\gamma,K^+)\Lambda$ is 4.2 ± 0.6, which is in good agreement with a calculation using a semiclassical model.

PACS number(s): 25.20.Lj, 21.80.a

Nuclear reactions including a strangeness degree of freedom, such as (K^-,π^-), (π^+,K^+), and (γ,K^+), leave a strangeness quantum number $S=-1$ in a nucleus converting a nucleon (N) into a hyperon (Λ or Σ). The creation of a hyperon in a nucleus offers an important opportunity to study effective nucleon-hyperon interactions through observations of hypernuclei and quasifree (QF) hyperon productions. Until now, hadronic strangeness exchanging (K^-,π^-) [1,2] and associated strangeness producing (π^+,K^+) [3–6] reactions have been used extensively to study the production and decay of hypernuclei. In particular, the recent spectroscopic observations using (π^+,K^+) have been employed to clarify the shell structure of the Λ hypernuclei [3].

The Λ-producing (γ,K^+) reactions are believed to be complementary to (K^-,π^-) and (π^+,K^+) which selectively excite natural parity states. The dominance of spin-flip amplitudes in (γ,K^+) near threshold enables us to observe spin multiplets in the Λ hypernuclear states [7–9]. Furthermore, the mean-free paths both of γ and K^+ in the nuclear medium are relatively long compared to those of $\pi^\pm$ and K^-. This feature makes it possible to probe the behavior of protons and Λ in the nuclear interior with less distortion. In order to arrive at a complete description of Λ in nuclei, results of hadronic probes must be combined with observations from Λ-producing electromagnetic processes.

In spite of the importance of (γ,K^+) measurements on nuclear targets, they have not been carried out due to a lack of suitable facilities. Since the cross section of (γ,K^+) in the threshold region is expected to be about one hundred times smaller than that of (π^+,K^+) in the same kinematical conditions [8], high duty cycle and high intensity electron beams are necessary to permit accurate (γ,K^+) observations.

This experiment is the first measurement of (γ,K^+) on nuclei (^{12}C) using a tagged photon beam. We present the differential cross section as a function of the incident photon energy E_γ and show the dominance of a QF Λ-producing $^{12}C(\gamma,K^+)$ reaction (QF-K^+) process. The experimental results are compared with a QF-K^+ calculation and a semiclassical model. The behavior of the (γ,K^+) reaction in the nuclear medium near threshold is also discussed.

*Present address: Nissan Motor Co. Ltd., Yokosuka 237, Japan.

†Present address: Research Institute for Nuclear Medicine and Biology, Hiroshima University, Hiroshima 734, Japan.

‡Present address: ALPS Electric Co. Ltd., Tokyo 145, Japan.

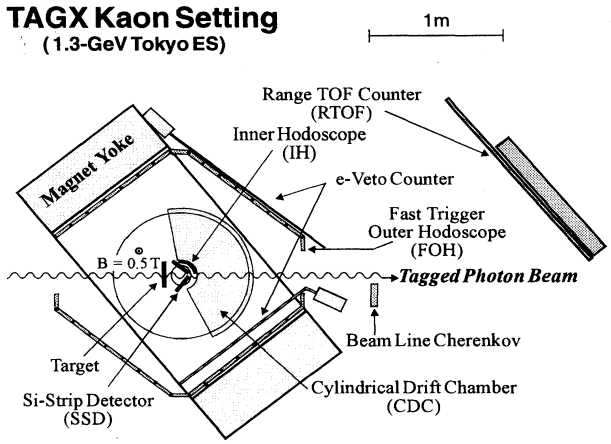

FIG. 1. Plan view of the spectrometer configuration for the $^{12}C(\gamma,K^+)$ experiment.

The experiment (ES132) was carried out at the 1.3-GeV Electron Synchrotron Laboratory of the Institute for Nuclear Study (INS), the University of Tokyo. The 1.2-GeV electron beam from the Synchrotron was extracted to the photon tagging channel with ~10% duty factor, and produced bremsstrahlung photons in a 100-μm-thick platinum radiator. The photons were tagged over the energy range of $0.8 \leq E_\gamma \leq 1.1$ GeV with $\Delta E_\gamma = \pm 5$ MeV (RMS) by bremsstrahlung-recoil electrons whose momenta were analyzed by a magnetic spectrometer (Tagger) [10]. The overall tagged photon flux was $\sim 4.5 \times 10^5\,\gamma$/s. A lead collimator (15 mm diameter $\times$1000 mm) and a sweep magnet were employed to cut off the beam halo and low momentum $e^\pm$. The photons irradiated a 1.49-g/cm^2-thick graphite target which was placed 77 mm upstream along the beam line from the detector center. The photon tagging efficiency, which was periodically monitored with a lead glass Čerenkov counter, was typically 80% at $E_\gamma = 1.1$ GeV.

Photoproduced charged particles were detected by a magnetic spectrometer (TAGX) [10,11] which consists of a dipole magnet, two cylindrical drift chambers (CDC) placed in a magnetic field, and inner (IH) and outer scintillation-counter hodoscopes (OH). As shown in Fig. 1, one CDC was placed at the forward direction in order to increase the acceptance at small angles. Additionally, a time-of-flight wall (RTOF), which works as a range telescope, was installed. Two sets of Silicon Strip Detectors (SSD) were placed in front of IH to extend the tracking points of charged particles. These additional counters were utilized to achieve enough separation to select K^+. They covered the angular ranges of $10° \leq \theta_{\rm lab} \leq 40°$ on the left-hand side and $0° \leq \theta_{\rm lab} \leq 30°$ on the right-hand side.

The momenta of positively charged particles were determined from the curvatures of the reconstructed tracks in CDC. The SSD hit positions were used to improve their momentum determination accuracy. Velocities were obtained from the time of flight (TOF) between IH and RTOF. A typical momentum and time resolutions were $\Delta p/p \approx 0.06$ (RMS) and $\Delta t/t \approx 0.04$ (RMS) for protons of 0.4 GeV/c, respectively. The distributions of the charged particle mass (M) are shown in Fig. 2 for the two kinematical ranges: (a) [$1.05 \leq E_\gamma \leq 1.10$ (GeV) and $0.5 \leq p \leq 0.6$ (GeV/c)], and

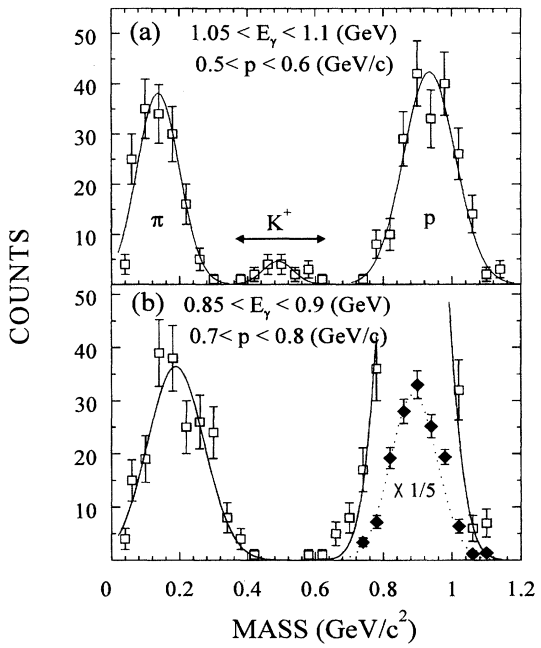

FIG. 2. Mass distributions of positively charged particles for two kinematical regions; (a) K^+ can be created, and (b) any (γ,K^+) reactions on ^{12}C are not kinematically allowed. Squares and solid lines show the data and the Gaussian fits, respectively. Diamonds and a dotted line in (b) represent their 1/5 values in $0.7 \leq M \leq 1.1$ GeV/c^2.

(b) [$0.85 \leq E_\gamma \leq 0.90$ (GeV) and $0.7 \leq p \leq 0.8$ (GeV/c)]. Three peaks centered at $M = 0.14$, 0.49, and 0.94 (GeV/c^2) in Fig. 2(a) correspond to π^+, K^+, and protons, respectively. On the other hand, there are negligible small entries in the K^+ mass region in (b) where any (γ,K^+) on ^{12}C are kinematically suppressed. We determined the K^+ yield by summing up the counts in the mass range of $M = 0.49 \pm 0.09$ GeV/c^2 ($\pm 2\sigma$ width). The probability of π^+ and protons contaminating into the identified K^+ was estimated to be less than 5% for the region (a).

From the inclusive K^+ yield and an estimation of the detector acceptance which includes the solid angle and the detection efficiency determined by a Monte Carlo simulation, we obtained double-differential cross sections $(d^2\sigma/d\Omega dp)$ above the detector threshold of $p^{(\rm dt)} = 240$ MeV/c. Differential cross sections can be obtained from an integration of $d^2\sigma/d\Omega dp$ as

$$\left(\frac{d\sigma}{d\Omega}\right)_{\rm lab} = (1+C)\int_{p^{(\rm dt)}} \frac{d^2\sigma}{d\Omega dp}\,dp, \qquad (1)$$

where the factor C corrects $(d\sigma/d\Omega)_{\rm lab}$ for the integration of $d^2\sigma/d\Omega dp$ below $p^{(\rm dt)}$. The K^+ momentum distribution for each E_γ bin was fitted by a QF-K^+ calculation, in which the proton momentum distributions in the s and p shell of ^{12}C were taken from the results of the $^{12}C(e,e'p)$ reaction [12]. The cross sections of the elementary $p(\gamma,K^+)\Lambda$ reaction were obtained by smoothing the experimental data [13]. C was estimated by an extrapolation of data above $p^{(\rm dt)}$ with

TABLE I. The estimated factor C to correct the K^+ yield for events below the K^+ detection threshold.

E_γ (GeV)	0.825	0.875	0.925	0.975	1.025	1.075
C	0.43	0.25	0.16	0.12	0.11	0.08

the assumption of QF-K^+. Estimated values of C as a function of E_γ, typically 11% at $E_\gamma=1$ GeV, are presented in Table I. This extrapolation gives an upper limit of $(d\sigma/d\Omega)_{\rm lab}$. When the amount of the coherent K^+ production leaving the hypernuclei is not small enough, it gives an over correction on $(d\sigma/d\Omega)_{\rm lab}$.

The obtained $(d\sigma/d\Omega)_{\rm lab}$ for $^{12}C(\gamma,K^+)$ at $10°\leqslant\theta_{\rm lab}\leqslant 40°$ are shown in Fig. 3 as a function of E_γ. The $p(\gamma,K^+)\Lambda$ cross sections [13], which are multiplied by a factor of 4 at the corresponding kinematical range, are plotted together for the comparison. The vertical bars denote the statistical errors. The systematic errors in the absolute magnitude of $(d\sigma/d\Omega)_{\rm lab}$ are estimated to be less than 9%. Triangles show $(d\sigma/d\Omega)_{\rm lab}$ without the correction by Eq. (1). They give the lower limit of the experimentally obtained cross sections if there is no background contribution from π or protons. The lines in Fig. 3 represent the Monte Carlo calculations of QF-K^+ described above. Dotted and dashed lines represent the contributions of two protons in the s shell and four protons in the p shell, respectively. The solid line shows the sum of these two contributions. Their absolute magnitudes are determined by normalizing the sum to data. Since the E_γ dependence of the $^{12}C(\gamma,K^+)$ cross section behaves similarly to that of $p(\gamma,K^+)\Lambda$ as a whole, the QF-K^+ process seems to be predominant above $E_\gamma\sim 1.0$ GeV. It can be seen that the nuclear Fermi motion causes the K^+ yield to rise more slowly near the $p(\gamma,K^+)\Lambda$ threshold of $E_\gamma^{(\rm th)}=0.91$ GeV than the elementary process. It should be noted that a sizable K^+ yield below $E_\gamma^{(\rm th)}$ after the subtraction of the QF contribution can be naturally explained by the existence of the coherent K^+ production process.

The missing mass M_x for $^{12}C(\gamma,K^+)X$ is given by

$$M_x=\sqrt{(k+M_C-(p^2+M_K^2)^{1/2})^2-(\mathbf{k}-\mathbf{p})^2}, \qquad (2)$$

where $\mathbf{k}$ and $\mathbf{p}$ are momenta of γ and K^+, and M_C and M_K represent masses of ^{12}C and K^+, respectively. The M_x distributions are shown in Fig. 4. The curves in (b) represent the results of the QF calculations. A broad peak centered at $M_x=11.5$ GeV/c^2 is reproduced well by the sum of QF-K^+ on protons both in s and p shells. One finds, however, an excess of the data above the QF calculation in the missing mass region below 11.4 GeV/c^2, where the bound Λ states of $^{12}_{\Lambda}B$ are expected. An integrated differential cross section over this region, which is obtained by a Gaussian fit shown by a dot-dashed line in Fig. 4, is 0.21 ± 0.05 μb/sr after subtraction of the QF-K^+ background. The theoretical value by Sotona *et al.* [8] for the sum of the bound Λ region ($\leqslant$15 MeV in the excitation energy of $^{12}_{\Lambda}B$) is $d\sigma/d\Omega=0.18$ μb/sr. From this agreement, it is satisfactory to consider that the yield in $11.2\leqslant M_x\leqslant 11.4$ GeV/c^2 corresponds to the Λ bound states. They mainly consist of the unnatural parity states which are predicted to be strongly excited in the present E_γ region [7,8]. Thus, the cross section for the (γ,K^+) reaction in the threshold region can be understood as a sum of QF-K^+ and a small ($\leqslant$10%) bound Λ contribution.

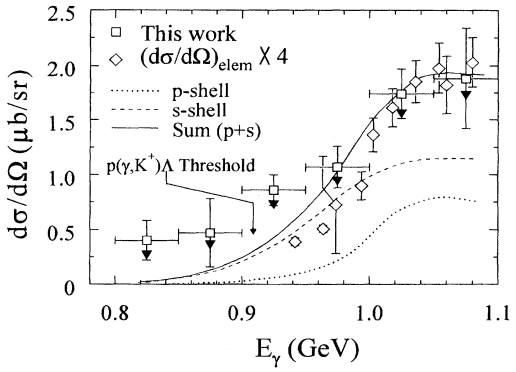

FIG. 3. Differential cross sections for $^{12}C(\gamma,K^+)$ as a function of E_γ. Squares and triangles show the experimental results with and without the correction of the unobserved region (see text). Diamonds represent the elementary $p(\gamma,K^+)\Lambda$ cross sections multiplied by a factor of 4 for the comparison. Lines show the result of the Monte Carlo calculation for QF-K^+ (see text).

The differential cross section of QF-K^+ can be written as [14]

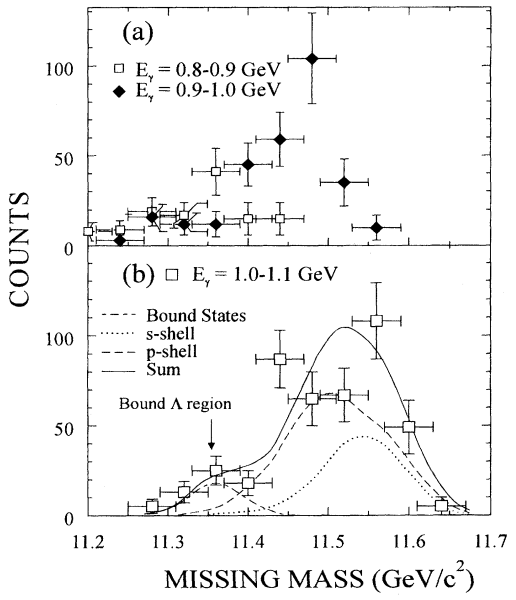

FIG. 4. Missing mass (M_x) distributions of the $^{12}C(\gamma,K^+)$ reaction at (a) $0.8\leqslant E_\gamma\leqslant 0.9$ GeV (squares) and $0.9\leqslant E_\gamma\leqslant 1.0$ GeV (diamonds) and (b) $1.0\leqslant E_\gamma\leqslant 1.1$ GeV. The bump around $M_x\sim 11.5$ GeV/c^2 corresponds to the missing mass of QF-K^+ (see text). Lines show the results of the Monte Carlo calculation (see text). The arrow indicates the mass of the $^{12}_{\Lambda}B$ ground state. The dot-dashed line shows the fitting of the bound region.

$$\left(\frac{d\sigma}{d\Omega}\right)_{\text{nucl}} = \int \left(\frac{d^2\sigma}{d\Omega dp}\right)_{\text{nucl}} dp \tag{3a}$$

$$= \left(\frac{d\sigma}{d\Omega}\right)_{\text{elem}} \int \alpha R(q,\omega) \frac{d\omega}{dp}\, dp \tag{3b}$$

$$= \left(\frac{d\sigma}{d\Omega}\right)_{\text{elem}} Z_{\text{eff}}, \tag{3c}$$

where $(d\sigma/d\Omega)_{\text{nucl}}$ and $(d\sigma/d\Omega)_{\text{elem}}$ are the differential cross sections for the nuclear and proton target, respectively. $R(q,\omega)$ is the nuclear response function as a function of the momentum transfer q and the energy transfer ω, and α is given with masses of a Λ and a proton as $\alpha^2=(M_\Lambda - M_p)/2M_p$. The quantity Z_{eff} refers to an effective number of protons which can be interpreted as the number of protons participating in the K^+-producing process, and includes the effects of absorptions both in the entrance and exit channels and the magnitude of the elementary transition amplitudes in the nuclear medium. From the Eq. (3c), Z_{eff} can be determined experimentally as a ratio of $(d\sigma/d\Omega)^{(\text{exp})}_{\text{nucl}}$ to $(d\sigma/d\Omega)^{(\text{exp})}_{\text{elem}}$. We obtained $Z^{(\text{exp})}_{\text{eff}}=4.2 \pm 0.6$ by comparing the present $(d\sigma/d\Omega)^{(\text{exp})}_{\text{nucl}}$ at $1.0 \leqslant E_\gamma \leqslant 1.1$ GeV and the $(d\sigma/d\Omega)^{(\text{exp})}_{\text{elem}}$ in the equivalent kinematical region [13].

In the framework of the eikonal approximation (EIK), Z_{eff} for $^{12}\text{C}(\gamma,K^+)$ is expressed for nuclear density $\rho(r)$, and incoming $[\chi^+_\gamma(\mathbf{r})]$ and outgoing $[\chi^-_{K^+}(\mathbf{r})]$ distorted waves as [14,15],

$$Z_{\text{eff}} = \tfrac{1}{2}\int \rho(r)|\chi^+_\gamma(\mathbf{r})|^2 |\chi^-_{K^+}(\mathbf{r})|^2 d^3\mathbf{r}$$

$$\approx \tfrac{1}{2}\int \rho(r)\left|\exp\left[i\mathbf{pr} - \int_{-\infty}^{z} \frac{\sigma^{(\text{tot})}_{\gamma N}}{2}\rho(r)dz\right]\right|^2 \tag{4a}$$

$$\times \left|\exp\left[-i\mathbf{pr} + \int_{z}^{\infty} \frac{\sigma^{(\text{tot})}_{K^+N}}{2}\rho(r)dz\right]\right|^2 d^3\mathbf{r}, \tag{4b}$$

where $\sigma^{(\text{tot})}_{\gamma N}=0.2$ mb and $\sigma^{(\text{tot})}_{K^+N}=12.0$ mb are the total $\gamma+N$ and K^++N cross sections taken from Ref. [16]. The evaluation of this approximation with a constant nuclear density $\rho=0.18$ fm^{-3} gives $Z_{\text{eff}}=3.9$ for $^{12}\text{C}(\gamma,K^+)$. A recent measurement of the total K^+ absorption in ^{12}C suggests that the attenuation of K^+ in the nuclear medium is about 10% larger than that expected from free K^+-N scattering [17]. When we use the modified K^+-N total cross section in ^{12}C, $Z_{\text{eff}}=3.5$ is obtained. The difference between the calculation is within the experimental error, when nuclear medium effects on K^+ propagation are included.

In conclusion, we measured the differential cross section of the $^{12}\text{C}(\gamma,K^+)$ reaction in the subthreshold region of $p(\gamma,K^+)\Lambda$ together with the region just above the threshold. The data above $E_\gamma=1.0$ GeV are reproduced by a QF-K^+ calculation with the experimentally known proton momentum distributions except for the low missing mass region of $M_x \leqslant 11.4$ GeV/c^2. In this region, the data are explained by the $^{12}_{\Lambda}$B excitation from the consistency between the experimental value and the predicted one. The effective number of protons $Z^{(\text{exp})}_{\text{eff}}=4.2\pm0.6$ in $^{12}\text{C}(\gamma,K^+)$ is in good agreement with a calculation in terms of EIK. From these results, we also conclude that (γ,K^+) have been demonstrated to be a useful tool to probe the nuclear interior. Detailed (γ,K^+) measurements both on the proton and nuclear targets are required for further discussions of Λ in nuclei.

The authors are indebted to Prof. T. Motoba for helpful discussions. We are also grateful to Prof. S. Yamada for his support throughout the present study. We wish to thank Prof. I. Endo, Prof. H. Okuno, Prof. K. Yoshida, Dr. M. Koike, Dr. K. Niki, Mr. H. Ifuku, Mr. T. Sasaki, and Mr. H. Uchida for their helpful collaboration in the testing stage of the experiment. K.M. is thankful for critical readings of the manuscript and for helpful discussions by Dr. B. Mecking. Part of this research was financially supported by Grant-in-Aid No. 02452019 for Scientific Research from the Ministry of Education, Science and Culture of Japan. Data analyses have been done with FACOM M-780 (Scientific Computational Program No. C106 and C115) of the INS computer room.

[1] G. C. Bonazzola, T. Bressani, E. Chiavassa, G. Dellacasa, A. Fainberg, M. Gallio, N. Mirfakhrai, A. Musso, and G. Rinaudo, Phys. Rev. Lett. **34**, 683 (1975); W. Brückner *et al.*, Phys. Lett. **79B**, 157 (1978).

[2] R. E. Chrien *et al.*, Phys. Lett. **89B**, 31 (1979).

[3] C. Milner *et al.*, Phys. Rev. Lett. **54**, 1237 (1985); P. H. Pile *et al.*, *ibid.* **66**, 2585 (1991); T. Hasegawa *et al.*, *ibid.* **74**, 224 (1995).

[4] M. Akei *et al.*, Nucl. Phys. **A534**, 478 (1991).

[5] S. Ajimura *et al.*, Nucl. Phys. **A547**, 47c (1992).

[6] K. Itonaga, T. Motoba, O. Richter, and M. Sotona, Phys. Rev. C **49**, 1045 (1994).

[7] S. S. Hsiao and S. R. Cotanch, Phys. Rev. C **28**, 1668 (1983).

[8] M. Sotona, K. Itonaga, T. Motoba, O. Richter, and J. Žofka, Nucl. Phys. **A547**, 63c (1992).

[9] C. Bennhold, Nucl. Phys. **A547**, 79c (1992).

[10] K. Niki, S. Kasai, S. Endo, A. Imanishi, K. Maruyama, and C. Rangacharyulu, Nucl. Instrum. Methods **A294**, 534 (1990).

[11] TAGX Collaboration, M. Asai *et al.*, Phys. Rev. C **42**, 837 (1990).

[12] J. Mougey, M. Bernheim, A. Bussière, A. Gillebert, Phan Xuan Hô, M Priou, D. Royer, I. Sick, and G. J. Wagner, Nucl. Phys. **A262**, 461 (1976).

[13] R. A. Adelseck and B. Saghai, Phys. Rev. C **42**, 108 (1990).

[14] C. B. Dover, L. Ludeking, and G. E. Walker, Phys. Rev. C **22**, 2073 (1980).

[15] H. Bando and T. Motoba, Prog. Theor. Phys. **76**, 1321 (1986).

[16] Particle Data Group, Phys. Lett. B **239**, III78,80 (1990).

[17] R. A. Krauss *et al.*, Phys. Rev. C **46**, 655 (1992).